BJRS
BRAZILIAN JOURNAL OF RADIATION SCIENCES

doi.org/10.15392/2319-0612.2026.3053
Braz. J. Radiat. Sci., Rio de Janeiro
2026, 14(2) | 01-26 | e3053
Editor(s): Dr. (Prof.) Bernardo Maranhão Dantas
Dr. (Prof.) Alfredo L. Ferreira Filho
Dr. (Prof.) Ademir de Jesus Amaral
Submitted: 2026-01-23
Accepted: 2026-05-18

Original Article

Assessment of Terrestrial Radionuclides and Radiological Risk within Indigenous Construction Materials: A Case Study from the Liwale District, Tanzania

Mammba[a*], H. P.; Matulanya[b], M. A.

[a] Tanzania Atomic Energy Commission, Southern Zone, Fery Area, Mtwara, Tanzania.
[b] Tanzania Atomic Energy Commission, Central Zone, P. O. Box 1585, Dodoma, Tanzania.

*Correspondence: peter.huruma2011@gmail.com

Abstract: Prolonged indoor exposure to radiation presents a public health concern, primarily due to building materials containing significant concentrations of natural radionuclides. This study was initiated in response to a documented case of elevated indoor gamma radiation in the Liwale District. The research aims to assess natural radioactivity levels in building materials sourced from this district, which is characterized by Hypoluvic Arenosols and Profondic/Arenic Luvisols derived from continental Neogene sandstone deposits, and to evaluate their potential radiological hazards. The radionuclide levels in 25 samples comprising sand, clay, and gravel were analyzed using a gamma-ray spectrometer coupled with a high-purity germanium (HPGe) detector. The average activity concentrations of ^{226}Ra, ^{232}Th, and ^{40}K were 40.8±2.5 Bq kg^{-1}, 114.9±4.1 Bq kg^{-1}, and 311.9±14.5 Bq kg^{-1}, respectively; Whilst ^{40}K levels were typical, the values for ^{226}Ra and ^{232}Th exceeded the UNSCEAR world averages. Moreover, average values for radiological hazard indices were: Ra_{eq}, 229.1±9.6 Bq kg^{-1}; H_{ex}, 0.6; I, 0.8, and E_{ff}, 0.5 mSv y^{-1}. Notably, the average values of all indices were within their internationally recommended limits, indicating a low overall radiological risk. Nevertheless, 20% of the samples (5 out of 25) exceeded the safety thresholds for Ra_{eq}, H_{ex}, and I, whilst 16% (4 out of 25) surpassed the limit for E_{ff}. This signifies potential lithogenic hazards associated with the use of these building materials. Therefore, this study strongly recommends implementing stringent regulatory screening and control measures for local building materials sourced from these specific geological formations.

Keywords: natural radionuclides, indoor radiation hazards, building materials.

doi.org/10.15392/2319-0612.2026.3053
Braz. J. Radiat. Sci., Rio de Janeiro
2026, 14(2) | 01-26 | e3053
Editor(s): Dr. (Prof.) Bernardo Maranhão Dantas
Dr. (Prof.) Alfredo L. Ferreira Filho
Dr. (Prof.) Ademir de Jesus Amaral
Submitted: 2026-01-23
Accepted: 2026-05-18

Évaluation des Radionucléides Terrestres et du Risque Radiologique dans les Matériaux de Construction Indigènes : Une Étude de Cas du District de Liwale, Tanzanie

Résumé: L'exposition prolongée aux rayonnements ionisants en milieu intérieur constitue un enjeu majeur de santé publique, principalement en raison de la présence de radionucléides naturels dans les matériaux de construction. Cette étude a été entreprise à la suite de la documentation de niveaux élevés de rayonnement gamma dans le district de Liwale. L'objectif est d'évaluer la radioactivité naturelle et les risques radiologiques associés aux matériaux de construction issus de cette région, caractérisée par des Arénosols hypoluviques et des Luvisols profondiques/aréniques dérivés de dépôts de grès néogènes continentaux. Vingt-cinq échantillons de sable, d'argile et de gravier ont été analysés par spectrométrie gamma à l'aide d'un détecteur au germanium de haute pureté (HPGe). Les concentrations d'activité moyennes mesurées pour le ^{226}Ra, le ^{232}Th et le ^{40}K étaient respectivement de 40.8±2.5 Bq kg^{-1}, 114.9±4.1 Bq kg^{-1} et 311.9±14.5 Bq kg^{-1}. Bien que les niveaux de ^{40}K soient conformes aux normes, les concentrations de ^{226}Ra et de ^{232}Th dépassent les moyennes mondiales de l'UNSCEAR. L'évaluation des indices de risque radiologique indique des valeurs moyennes (Ra_{eq}, 229.1±9.6 Bq kg^{-1}; H_{ex}, 0.6; I, 0.8, et E_{ff}, 0.5 mSv an^{-1}) situées en deçà des limites internationales recommandées, suggérant un risque globalement faible. Toutefois, une analyse individuelle révèle que 20 % des échantillons (5 sur 25) excèdent les seuils de sécurité pour Ra_{eq}, H_{ex}, et I, tandis que 16 % (4 sur 25) dépassent la limite de dose efficace annuelle (E_{ff}). Ces résultats mettent en évidence des risques lithogéniques potentiels liés à l'utilisation de ces matériaux de construction. En conséquence, cette étude préconise la mise en œuvre rigoureuse de mesures réglementaires de contrôle et de dépistage des matériaux de construction issus de ces formations géologiques spécifiques.

Mots-clés: radionucléides naturels, risques radiologiques intérieurs, matériaux de construction.

1. INTRODUCTION

All living organisms are consistently exposed to both natural and anthropogenic sources of ionizing radiation. On a global scale, approximately 8% of this exposure originates from cosmic radiation, while the remaining 82% is attributed to the decay of naturally occurring radioactive materials (NORM) in Earth's crust [1-3]. The most common NORM include radionuclides from the decay series of uranium-238 (^{238}U) and thorium-232 (^{232}Th), as well as potassium-40 (^{40}K) [4]. The concentrations of these radionuclides vary significantly with local geological formations and geochemical properties [3,5]; for instance, igneous rocks such as granite typically exhibit higher NORM concentrations than sedimentary materials such as clay or limestone [6]. While NORM is naturally present in the environment, anthropogenic activities, including mining, mineral processing, and the use of phosphate fertilizers, can further elevate these concentrations, thereby increasing radiological risk to both the environment and human health [7,8].

Building materials, frequently sourced from natural geological formations, naturally contain varying levels of NORM. Since modern populations spend approximately 80% of their time indoors, ionizing radiation emitted by these materials (integrated into walls, floors, and ceilings) is the primary source of both external and internal radiation exposure in dwellings [2,3,9-11]. External exposure is predominantly caused by direct gamma radiation, whereas internal exposure arises from the inhalation of radon (^{222}Rn) and thoron (^{220}Rn) gases byproducts of the ^{238}U and ^{232}Th series, respectively, and their short-lived progeny [5,9]. Epidemiological evidence suggests that prolonged exposure to such indoor radiation is linked to an increased risk of cancer and cardiovascular diseases [10,12-16]. Specifically, the long-term inhalation of radon gas is a well-documented cause of damage to bronchial epithelial cells, leading to lung cancer [17-20]. Consequently, the systematic characterization of NORM

in building materials is essential for managing public health risks and establishing baselines for monitoring changes in environmental radioactivity [2,3,7].

Despite the importance of such monitoring, localized data remains scarce in many developing regions. In 2023, internal technical assessments conducted by the Tanzania Atomic Energy Commission (TAEC) identified anomalously high indoor gamma radiation levels in several residential buildings in the Liwale District of the Lindi Region, southern Tanzania [21]. Preliminary inspections suggested that these emissions originated from the NORM content of building walls; however, these assessments were restricted to a small number of suspected sites. To date, a comprehensive radiological characterization of the soil and building materials across the Liwale District has not been documented in the peer-reviewed literature.

To address this knowledge gap, the present study assesses the activity concentrations of ^{226}Ra, ^{232}Th, and ^{40}K in building materials sourced from various mine sites and local markets within the Liwale District. These materials are primarily derived from the region's Hypoluvic Arenosols and Luvisols, which originate from continental Neogene sandstone deposits. Using p-type coaxial high-purity germanium (HPGe) gamma-ray spectrometry, this research evaluates radiological risks using internationally recognized indices, including radium equivalent activity (Ra_{eq}), external radiation hazard index (H_{ex}), activity concentration index (I), and Annual effective dose (E_{ff}) [23-31]. These findings are critical for benchmarking local radioactivity against international safety standards and establishing the inaugural radiological baseline for building materials in this region.

2. MATERIALS AND METHODS

2.1. Study Area

The study was conducted in the Liwale District of the Lindi Region in Southern Tanzania (Figure 1). Geographically, the district is bounded by latitudes 8°17´30.12˝ S to 10°12´5.648˝ S, and longitudes 38°4´42.599˝ E to 37°24´25.03˝ E. As the largest administrative district in the Lindi Region, Liwale encompasses approximately 34,314 km² and supports a population of 107,711 residents [32].

From a pedological and geological perspective, the district is characterized by extensive tracks of deep, sandy soil profiles. These soils originate from continental Neogene sandstone deposits and are scientifically classified as predominantly Hypoluvic Arenosols, as well as Profondic and Arenic Luvisols [22]. While the local economy is predominantly driven by agriculture, specifically the production of cashew and cassava, the district's infrastructure relies heavily on lithogenic materials sourced from local quarries and primary extraction points. These sites were specifically targeted for sampling because they are the principal suppliers of construction aggregates and raw materials in the region. To ensure a focused assessment of indoor radiological risks, this research prioritizes the lithogenic pathway of radiation exposure, specifically characterizing construction materials rather than investigating the agricultural environment or dietary exposure.

Figure 1: Geographical distribution of sampling sites for clay, sand, and gravel in the Liwale District, Tanzania (n=25)

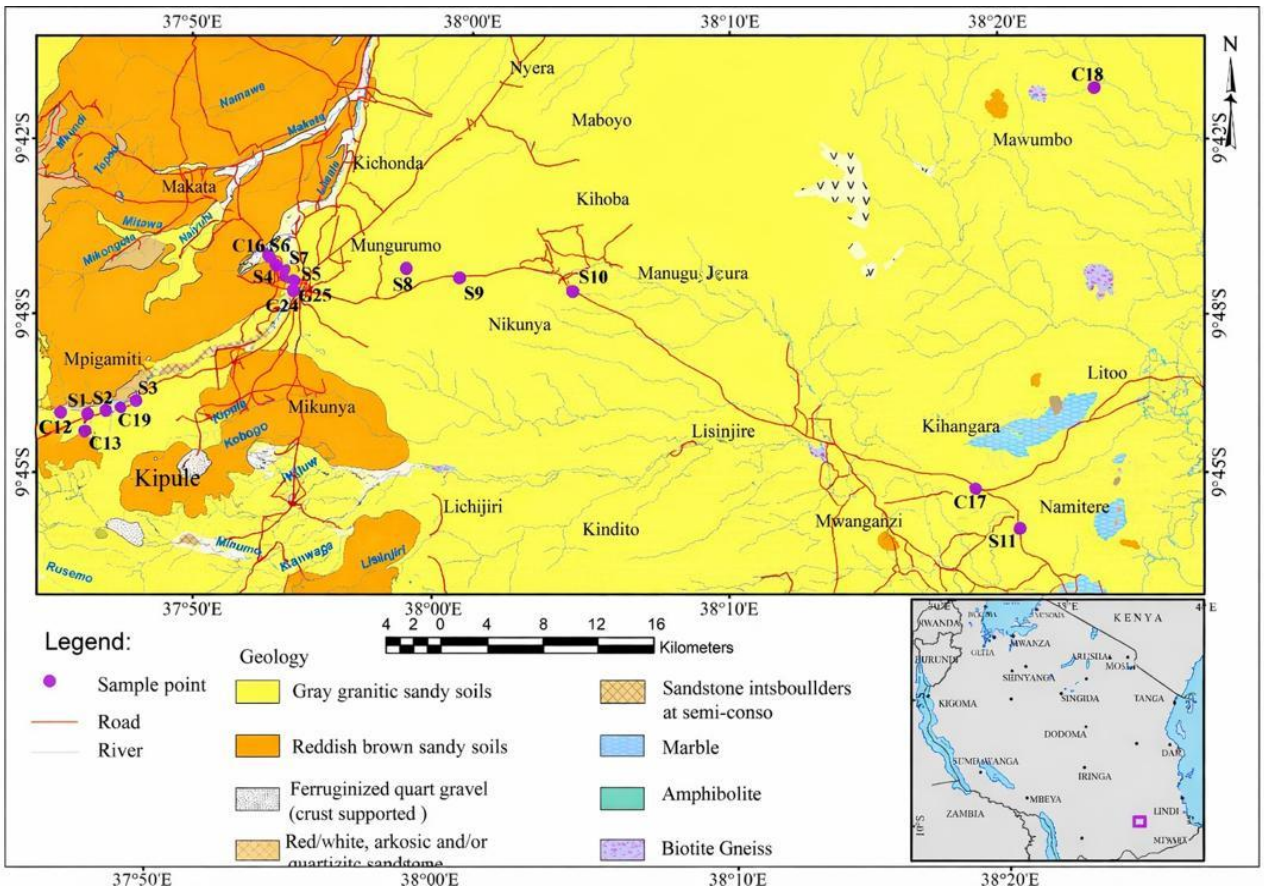

2.2. Sampling and Sample Preparation

A total of 25 samples, including sand, clay, and gravel, were collected using a simple random sampling technique from licensed mines and mineral suppliers across the Liwale District. These materials are representative of the region's characteristic soil formations, specifically the Hypoluvic Arenosols and Luvisols derived from sandstone deposits [22], which are the primary sources for local building aggregates. To obtain each sample, approximately 1.5 kg of material was excavated from a depth of 10–30 cm using a decontaminated shovel. The samples were immediately transferred into coded, airtight polythene bags to prevent cross-contamination and transported in waterproof containers to the TAEC laboratory for analysis.

In the laboratory, the samples were processed in a controlled environment where foreign organic matter (such as roots and pebbles) was manually removed. Each sample was

thoroughly homogenized to ensure a representative composite before being cataloged and weighed. The samples were then dried in an oven at 105 °C for approximately 24 hours, or until a constant weight was achieved, to ensure the complete removal of moisture and volatile organic matter [2,6,23,25,33]. Once cooled to room temperature, the dried materials were pulverized and sieved through a 1 mm mesh to achieve a uniform particle size.

For the radiological measurements, approximately 400 - 420 g of the sieved powder was transferred into clean cylindrical canisters. The dimensions of these canisters were selected to match the geometry of the certified reference materials (CRMs) used for system calibration. The canisters were hermetically sealed using a mechanical sealer and further wrapped in polythene tape to prevent the escape of radiogenic gases, particularly radon. The sealed units were then stored for a minimum of 30 days to allow radioactive secular equilibrium between ^{226}Ra and its short-lived progeny to be attained [2,5-7,34].

2.3. Radiometric Characterization and Instrumentation

The activity concentrations of ^{226}Ra, ^{232}Th, and ^{40}K were determined using a p-type coaxial high-purity germanium (HPGe) gamma ray spectrometer. The detector featured a relative counting efficiency of 20% and an energy resolution of 1.8 keV (FWHM) at the 1332 keV gamma ray emission of ^{60}Co. To maximize detection efficiency for low-level NORM activities, each sample canister was positioned directly onto the detector endcap.

The entire assembly was housed vertically within a cylindrical shield of high-purity lead 10 cm thick. To minimize backscattering effects and suppress characteristic lead X-rays (fluorescence) that could interfere with the low-energy region of the spectrum, the interior of the shield was lined with a graded layer of high-purity copper. This high-atomic-number shielding was employed to attenuate ambient background radiation and minimize interference from cosmic rays, thereby ensuring the high sensitivity required to assess radiological health risks effectively [7, 27, 34-36]. This analytical technique is consistent with established international protocols for monitoring radioactivity in environmental and construction materials [33].

2.4. Measurement Procedures and Activity Quantification

Prior to sample analysis, the ambient gamma background was established by measuring an empty, sealed canister under identical experimental conditions for the same duration as the samples. Following this, each building material sample was counted for approximately 12 hours (43,200 seconds) to ensure sufficient net counts for statistically significant photopeak analysis. Spectral acquisition and data processing were performed using Gamma Vision (2017) software.

Since the samples had attained secular equilibrium, the activity concentrations of ^{226}Ra were determined from gamma-ray photopeak energies of 609.2 keV (^{214}Bi) and 351.9 keV (^{214}Pb). The ^{232}Th concentrations were obtained by measuring the ^{228}Ac photopeak at 338.4 and 968.9 keV, and the ^{212}Pb photopeak at 238.6 keV. The concentration of ^{40}K was determined directly using its 1461.7 keV photopeak [36]. The activity concentrations were calculated by comparing the results with IAEA reference materials using the comparison method defined in Equation 1, as documented in established literature [7,36,37].

$$A_s = \frac{M_{ref}}{M_s} x \frac{N_s}{N_{ref}} \; x \; A_{ref} \tag{1}$$

Where A_s is the concentration of radionuclide in the collected sample (Bq kg^{-1}), M_{ref} is the weight of the standard sample (kg), M_s is the weight of the collected sample (kg), N_s is the net count of the photopeak area of the collected sample, N_{ref} is the net count of the photopeak area of the standard sample, and A_{ref} is the concentration of radionuclide of the standard sample (Bq kg^{-1}).

2.5. Radiological Hazards Indices

To assess the radiological risks associated with external gamma radiation emitted by radionuclides present in building materials, four radiological hazard indices were calculated.

2.5.1. Radium equivalent activity (Ra_{eq})

The radium equivalent activity, Ra_{eq}, is a widely used criterion for accounting for gamma-ray emission from ^{226}Ra, ^{232}Th, and ^{40}K, based on the assumption that 370 Bq kg^{-1} of ^{226}Ra, 259 Bq kg^{-1} of ^{232}Th, and 4,810 Bq kg^{-1} of ^{40}K produce the same gamma dose rate. The assumption considers that the distribution of these radionuclides in the soil is not uniform. Notably, the assumption uses ^{226}Ra instead of the uranium radionuclide (^{238}U) because ^{226}Ra is produced by the decay series of ^{238}U and accounts for 98.5% of the radiological effects of that series [7,17]. The activity concentration values of Ra_{eq} for the studied samples were calculated using Equation 2, as reported in the literature [3,5,7,16,25,33,36].

$$Ra_{eq} = 370\ \text{Bq kg}^{-1}\left(\frac{\text{A}_{\text{Ra}}}{370\ \text{Bq kg}^{-1}} + \frac{\text{A}_{\text{Th}}}{259\ \text{Bq kg}^{-1}} + \frac{\text{A}_{\text{K}}}{4810\ \text{Bq kg}^{-1}}\right)$$

$$\text{Or, } \text{Ra}_{\text{eq}} = \text{A}_{\text{Ra226}} + 1.43\text{A}_{\text{Th}} + 0.077\text{A}_{\text{K}} \qquad (2)$$

Where A_{Ra} is the activity concentration of ^{226}Ra in Bq kg^{-1}, A_{Th} is the activity concentration of ^{232}Th in Bq kg^{-1}, A_{K} is the activity concentration of ^{40}K in Bq kg^{-1}.

According to the literature, the Ra_{eq} value should be less than 370 Bq kg^{-1} for building materials to be considered safe, as this ensures the average annual effective dose remains within the acceptable limit (1 mSv y^{-1}) [12]. Although ICRP Publication 144 has recently updated external dose conversion factors, this criterion remains widely used to compare results with previous global studies [38].

2.5.2. External radiation hazard index (H_{ex})

The external radiation hazard index, H_{ex}, is a criterion used to assess indoor gamma dose rates resulting from external exposure to gamma radiation emitted by natural radionuclides in building materials. This index is crucial for evaluating the long-term safety of structures, as it ensures that radiation exposure remains within acceptable limits. The index is a dimensionless quantity derived from the expression of radium equivalent activity through the assumption that its maximum accepted value corresponds to the upper limit of Ra_{eq} of

370 Bq kg^{-1} [3,7]. The H_{ex} value must be less than unity to keep radiation hazards insignificant by keeping the average annual effective dose within the acceptable limit of <1 mSv y^{-1} [12,39]. The index is calculated using the criterion specified in Equation 3 [7,29,40].

$$H_{ex} = \frac{A_{Ra}}{370\ Bq\ kg^{-1}} + \frac{A_{Th}}{259\ Bq\ kg^{-1}} + \frac{A_K}{4810\ Bq\ kg^{-1}}$$

$$\text{Or, } H_{ex} = \frac{Ra_{eq}}{370\ Bq\ kg^{-1}} \quad (3)$$

Where Ra_{eq} is the radium equivalent activity in Bq kg^{-1}.

2.5.3. Activity concentration index (*I*)

The activity concentration index (*I*) provides a standardized framework for identifying building materials subject to regulatory oversight by monitoring the activity concentrations of ^{226}Ra, ^{232}Th, and ^{40}K [13]. Derived from the European Council Directive 2013/59/Euratom, this index is based on a conservative model in which the annual external gamma radiation dose contributed by building materials does not exceed the public limit of 1 mSv y^{-1}. For the safe use of bulk materials, such as aggregates, sand, and clay, the index value should be ≤1 [23,38]. The activity concentration index is calculated according to the formula presented in Equation 4:

$$I = \frac{A_{Ra}}{300\ Bq\ kg^{-1}} + \frac{A_{Th}}{200\ Bq\ kg^{-1}} + \frac{A_K}{3000\ Bq\ kg^{-1}} \quad (4)$$

Where; A_{Ra}, A_{Th}, and A_K are the activity concentrations of radionuclides ^{226}Ra, ^{232}Th and ^{40}K, respectively, expressed in $Bq\ kg^{-1}$.

2.5.4. Annual effective dose (E_{ff})

The Annual effective dose (E_{ff}) serves as another fundamental screening tool for the radiological assessment of construction materials containing radionuclides of natural origin. Used for regulatory purposes worldwide, the E_{ff} provides a risk-adjusted measure of the total body dose relative to the stochastic risks of cancer and hereditary effects, expressed in terms

of health detriment [38]. To quantify this exposure within the indoor environment, the E_{ff} is derived from the absorbed dose rate by incorporating an indoor occupancy factor and a conversion coefficient that translates the absorbed dose in air into the effective dose in human tissue. Consequently, the E_{ff} (mSv y^{-1}) is computed using the following formula:

$$E_{ff}(mSv\ y^{-1}) = D\ x\ T\ x\ 0_f\ xC_c\ x\ 10^{-6} \quad (5)$$

Where: (D) is the absorbed dose rate in nGy h^{-1}, (T) is the total hours in a year (8,760 $h\ y^{-1}$), (O_f) is the indoor occupancy factor, which equals to 0.8 (or 80%), (C_c) is the conversion coefficient from absorbed dose in air to effective dose in the human body for adults, which is equal to 0.7 $SvGy^{-1}$, and 10^{-6} is the factor to convert nGy to Gy and Sv to mSv as required by the units.

The absorbed dose rate (D) utilized in Equation 4 is determined by correlating the activity concentrations of the ^{238}U and ^{232}Th series, and ^{40}K in building materials with the resulting dose rate in air [12]. Relationship is expressed as:

$$D(nGy\ h^{-1}) = DC_{Ra}xA_{Ra} + DC_{Th}xA_{Th} + DC_{K}xA_{K} \quad (5)$$

Where, and A_{Ra}, A_{Th} and A_K are the activity concentrations (Bq kg^{-1}) of ^{226}Ra, ^{232}Th, and ^{40}K, respectively. The terms DC_{Ra}, DC_{Th}, and DC_K denote the specific dose-rate conversion factors for ^{226}Ra, ^{232}Th, and ^{40}K, with values of 0.462, 0.604, and 0.0417 nGy h^{-1} per Bq kg^{-1}, respectively [12].

Finally, the calculated value of E_{ff} is then compared against the internationally recommended safety limit of 1 mSv y^{-1} for public exposure [13].

3. RESULTS AND DISCUSSIONS

3.1. Activity Concentration of Radionuclides

The activity concentrations of ^{226}Ra, ^{232}Th, and ^{40}K in building materials from Liwale District are detailed in Table 1, which presents the minimum, maximum, and average values, along with their respective standard deviations (SD). The average activity concentrations of the radionuclides varied significantly across sample types. For ^{226}Ra, concentrations ranged from a minimum of (4.4±1.1 Bq kg^{-1}) in sand to a maximum of (119.1±3.6 Bq kg^{-1}) in gravel. A similar trend was observed for ^{232}Th, with the lowest concentration found in sand (12.6±7.6 Bq kg^{-1}) and the highest in gravel (446.7±8.5 $Bq\ kg^{-1}$). In contrast, ^{40}K displayed a different trend: its concentrations were lowest in gravel (12.3 ± 9.2 Bq kg^{-1}) and reached a maximum of 851.9 ± 24.2 Bq kg^{-1} in clay. As shown in Table 1, the average activity concentrations of ^{226}Ra, ^{232}Th, and ^{40}K in the studied building materials were 40.8±2.5 Bq kg^{-1}, 114.9±4.1 Bqkg^{-1}, and 311.9±14.5 Bq kg^{-1}, respectively. The average activity concentrations of ^{226}Ra and ^{232}Th in this study demonstrably exceed global average benchmarks of 32 Bq kg^{-1} for ^{226}Ra and 45 Bq kg^{-1} for ^{232}Th. This deviation suggests a potential localized enrichment or distinct geological influences contributing to the elevated levels of these radionuclides. Conversely, the average ^{40}K activity concentration aligns with the global average of 420 Bq kg^{-1} [12]. Further research is necessary to elucidate the precise mechanisms driving the observed disparities, which may include geological composition, soil genesis, and anthropogenic influences.

To contextualize the findings, the average activity concentrations of ^{226}Ra, ^{232}Th, and ^{40}K from the current study were compared with data from local regions and international studies, as summarized in Table 2. These values indicate the specific regions within the countries mentioned where samples were collected. The comparison results generally reveal that the radioactivity concentrations of building materials worldwide vary from one country to another but are mostly within the global average [12]. A regional comparison reveals that

the radionuclide concentrations of building materials in the current study are significantly higher than those reported in the Kinondoni District [7]. Furthermore, when benchmarked against regional studies from uranium-deposit areas, the activity concentration of ^{232}Th was notably higher than levels reported in the Manyoni and Namtumbo Districts [26,32]. While existing literature frequently correlates elevated radionuclide levels with anthropogenic activities, as observed in Nigerian oil extraction zones [35] and Namibian uranium mining towns [41], this correlation is not supported by the current study. Instead, given the absence of industrial activities known to increase soil radioactivity in the Liwale district, the observed radionuclide concentrations in building materials are likely geogenic in origin.

Table 1: Activity concentrations and radiological indices of building materials originating from Liwale District

Sample type	Sample ID	Activity Concentrations			Radiological Hazards Indices			
		^{226}Ra Bq kg^{-1}	^{232}Th Bq kg^{-1}	^{40}K Bq kg^{-1}	Ra_{eq} Bq kg^{-1}	H_{ex}	I	E_{ff} mSv y^{-1}
Sand	S1	66.3±4.1	66.9±2.7	173.7±12.7	175.4±9.5	0.5	0.6	0.4
	S2	56.3±2.5	229.8±3.7	328.6±13	410.2±8.2	1.1	1.4	0.9
	S3	111.6±4.7	435.0±7.4	675.1±23.6	785.6±15.9	2.1	2.8	1.7
	S4	46.3±2.7	127.4±4.5	477.2±18	265.3±9.8	0.7	1.0	0.6
	S5	4.4±1.1	18.4±4.2	13.2±1.7	31.8±5.9	0.1	0.1	0.1
	S6	26.9±2.3	64.6±3.8	81.8±12.7	125.6±8.1	0.3	0.4	0.3
	S7	98.1±4.0	341.4±7.9	759.6±26.9	644.7±15.7	1.7	2.3	1.4
	S8	72.8±3.0	237.5±6.2	528.1±20.1	453.1±12	1.2	1.6	1.0
	S9	23.6±1.6	45.0±1.31.3	409.0±13.9	110.2±4.6	0.3	0.4	0.3
	S10	20.0±2.0	48.6±3.1	265.0±13.6	97.7±7.1	0.3	0.4	0.2
	S11	9.5±6.6	12.6±7.6	115.9±7.9	35.1±17.7	0.1	0.1	0.1
Max.		111.6±3.6	435±8.5	759±24.2	785.6±15.9	2.1	2.8	1.4
Min.		4.4±1.1	12.6±7.6	13.2±9.2	31.8±5.9	0.1	0.1	0.1
Average on Sand		**48.7±3.1**	**147.9±4.8**	**347.9±14.9**	**287±10.4**	**0.8**	**1.0**	**0.6**

Sample type	Sample ID	Activity Concentrations			Radiological Hazards Indices			
		^{226}Ra Bq kg^{-1}	^{232}Th Bq kg^{-1}	^{40}K Bq kg^{-1}	Ra_{eq} Bq kg^{-1}	H_{ex}	I	E_{ff} mSv y^{-1}
Clay	C12	18.5±0.9	43.1±1.3	14.9±0.5	81.3±2.8	1.3	0.3	0.2
	C13	28.1±2.5	79.5±4.1	65.1±12.4	146.8±9.4	2.4	0.5	0.3
	C14	46.3±2.0	48.5±3.0	96.6±8.8	123.1±7	0.8	0.4	0.3
	C15	11.5±1.7	18.1±1.1	138.0±11.5	48±4.2	0.1	0.2	0.1
	C16	11.4±1.3	17.9±8.8	46.7±8.7	40±14.6	0.4	0.1	0.1
	C17	13.9±1.1	23.0±1.4	149.6±7.2	58.3±3.7	2	0.2	0.1
	C18	17.2±2.0	25.7±1.4	851.9±24.2	119.6±5.8	1.4	0.5	0.3
Max.		46.3±3.6	79.5±8.5	851.9±24.2	146.8±15.6	0.4	0.5	0.3
Min.		11.4±1.1	17.9±7.6	14.9±9.2	40.5±5.9	0.1	0.1	0.1
Average on Clay		**21±1.6**	**36.5±3**	**194.7±10.5**	**88.2±6.8**	**0.2**	**0.3**	**0.2**
Gravels	G19	37.4±1.4	68.8±1.6	12.3±9.2	136.8±4.4	0.3	0.5	0.3
	G20	26.9±2.3	22.3±1.2	81.8±12.7	65.1±5	0.2	0.2	0.1
	G21	38.8±2.4	124.7±4.9	253.0±14	236.6±10.4	0.5	0.8	0.5
	G22	33.5±2.2	100.9±4.7	360.1±19.6	205.6±10.5	0.5	0.7	0.4
	G23	47.2±3.0	133.3±4.6	464.8±19.9	273.6±11.1	0.6	1.0	0.6
	G24	33.4±2.5	93.3±4.1	775.2±24.1	226.5±10.2	0.5	0.8	0.5
	G25	119.1±3.6	446.7±8.5	661.2±24.7	808.9±17.7	1.8	2.9	1.7
Max		119.1±3.6	446.7±8.5	775.2±24.2	808.9±15.6	1.8	2.9	1.7
Min.		26.9±1.1	22.3±7.6	12.3±9.2	65.1±5.9	0.2	0.2	0.1
Average on Gravels		**48±2.5**	**141.4±4.2**	**372.6±17.9**	**279±9.9**	**0.6**	**1.0**	**0.6**
Total	**Max.**	**119.1±3.6**	**446.7±8.5**	**851.9±24.2**	**808.9±17.7**	**2.2**	**2.9**	**1.7**
	Min.	**4.4±1.1**	**12.6±7.6**	**12.3±9.2**	**31.8±5.9**	**0.1**	**0.1**	**0.1**
	Avg.	**40.8±2.5**	**114.9±4.1**	**311.9±14.5**	**229.1±9.6**	**0.6**	**0.8**	**0.5**

Table 2: The average activity concentrations of ^{226}Ra, ^{232}Th, and ^{40}K in Bq kg^{-1} of building materials from different locations around the world

Location and Country	Sample type	^{226}Ra	^{232}Th	^{40}K	Reference
Liwale District, **Tanzania**.	Sand, clay & gravel	40.80	114.90	311.90	Current study
Semnan province, **Iran**.	Sand and gravel	240	2.00	362	[2]
West Bank, **Palestine**.	Soil	-	19.50	113.30	[6]
Kinondoni District, **Tanzania**.	Clay	10.30	17.60	251.18	[7]
Manyoni District, **Tanzania**.	Soil	227.43	65.22	107.32	[25]
Guangyao Village, **South China**.	Soil	26.84	8.87	453.81	[26]
Himachal Pradesh, **India**.	Soil	57.34	82.22	135.75	[28]
Kota Tinggi town, **Malaysia**.	Soil	16.84	20.06	38.53	[29]
Namtumbo District, **Tanzania**.	Soil	36.27	33.80	555.87	[31]
Dhaka City, **Bangladesh**.	White sand	49.40	71.60	927.20	[33]
Oyo State Capital, **Nigeria**.	Soil	-	10.95	89.36	[35]
Abidjan District, **Côte d'Ivoire**.	Gravel	5.98	4.17	177.18	[37]
Erongo region, **Namibia**.	Soil	81.24	72.1	682	[41]
East coast of Tamil Nadu, **India.**	Soil	-	14.29	360.23	[42]
South Nile Delta, **Egypt**.	Soil	11.26	4.89	141.61	[43]
Maanshan – South Bay, **Taiwan**.	Soil	18.6	26.5	344.4	[44]
Istanbul region, **Turkey**.	Clay	39.3	49.6	569.5	[45]
Aden governorate, **Yemen**.	Soil	59.39	71.32	697	[46]
Qassim, **Saudi Arabia**.	Gravel	14.7	24.2	195	[47]
Nairobi City, **Kenya**.	Sand	-	290	831	[48]
Gumuz Region, **Ethiopia**.	Soil	-	45	420	[49]
Worldwide Average.	**Soil**	**32**	**45**	**420**	**[12]**

3.2. Assessment of the Radiological Hazards

To evaluate the potential radiological hazards associated with building materials from Liwale District, this study calculated four radiation hazard indices. These indices are the radium equivalent activity (Ra_{eq}), the external radiation hazard index (H_{ex}), the activity concentration index (I), and the annual effective dose (E_{ff}). The Ra_{eq} values for various material types are summarized in Figure 2, whilst Figure 3 provides a comparative analysis of the H_{ex}, I, and E_{ff} indices across the different material types.

Figure 2: Average radium equivalent activity (Ra_{eq}) across different building materials sources from the Liwale District. The red line represents the internationally recommended safety limit of 370 Bq kg^{-1}.

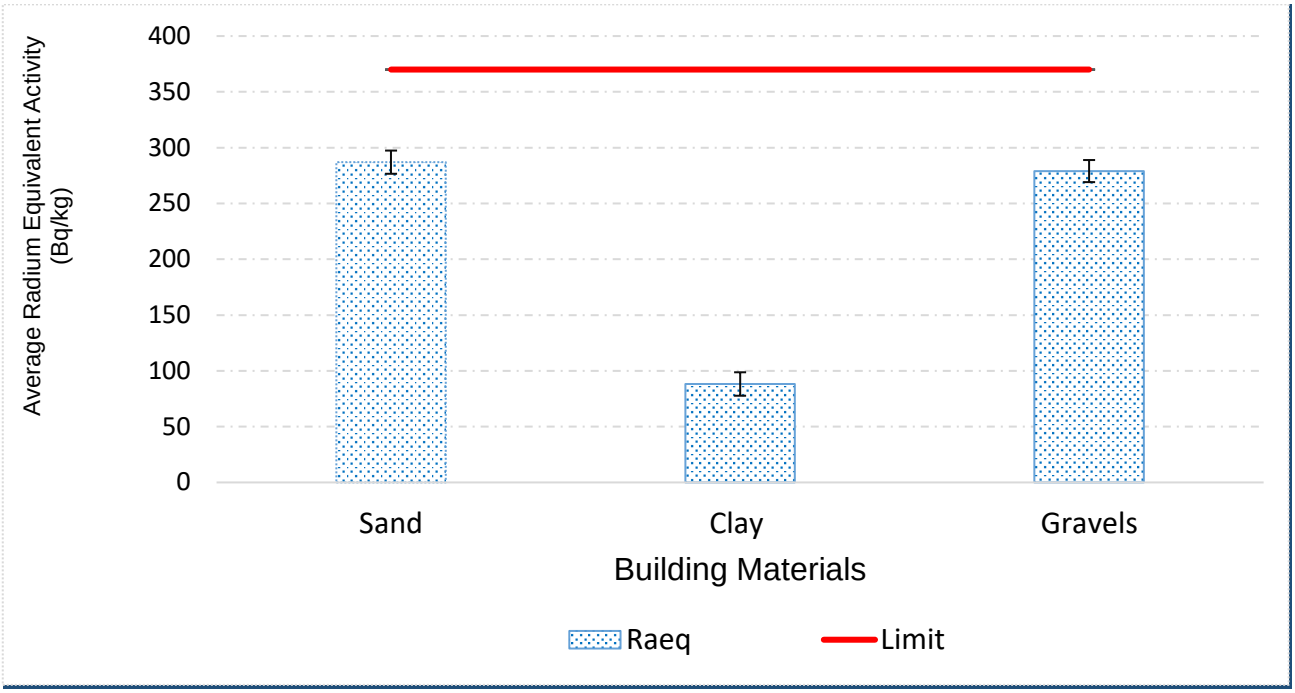

Figure 3: Comparative distribution of the average external hazard index (*Hex*), activity concentration index *(I*), and annual effective dose (*Eff*) by material type. The red line indicates the safety threshold of 1.0 (applicable to all three indices)

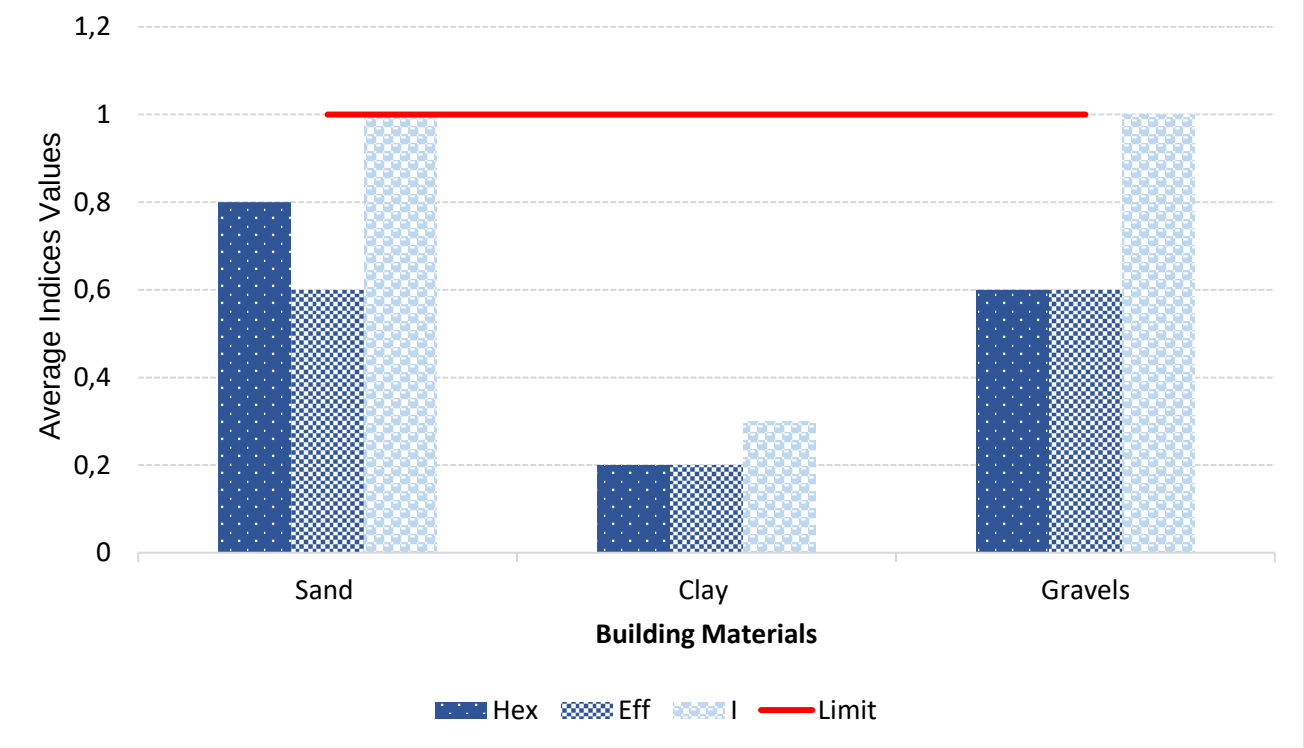

A. Radium equivalent activity (Ra_{eq})

As illustrated in Table 1(column 6) and visualized in Figure 2, the analysis of radium equivalent activity (Ra_{eq}) revealed substantial variation among the samples, with an average value of 229.1 ± 9.6 Bq kg^{-1}. Figure 2 highlights that whilst the average values for all three material categories remain below the internationally recommended safety limit of 370 Bq kg^{-1} [12], a notable disparity exists between the materials. Specifically, sand and gravel exhibited higher average Ra_{eq} values compared to clay. A detailed examination of individual data points reveals a significant radiological concern: 5 of the 25 samples (20%) exceeded this critical threshold, with 1 sample reaching a concentration of 808.9 ± 17.7 Bq kg^{-1}. This finding is of particular importance, as the non-compliant samples were identified as sand (n = 4) and gravel (n = 1). Given that these are primary constituents in concrete and other common construction applications, their unregulated use could lead to elevated indoor gamma radiation levels, thereby increasing the external radiation dose to occupants. Consequently, while the materials may be considered generally safe on average, the presence of these high activity levels underscores the need for systematic radiological screening of raw materials to mitigate potential health risks and ensure compliance with public safety standards.

B. External radiation hazard index (H_{ex})

The H_{ex} values for the studied samples ranged from 0.1 to 2.2, with an average of 0.6. As illustrated in the comparative plot (Figure 3), the H_{ex} average values of sand, clay and gravel remain well within the recommended safety criterion of 1, as stipulated by UNSCEAR [12]; this suggests a generally acceptable level of background radiation from these materials when assessed on an aggregate basis. Despite the reassuring average value, a critical finding of this study is the non-compliance of a notable subset of samples. Specifically, 5 of the 25 samples (20%) exhibited H_{ex} values exceeding the permissible limit. These elevated H_{ex} values were identified exclusively in sand and gravel samples. This result suggests that a substantial portion of the sand and gravel sources in the district may contribute to indoor gamma dose rates that surpass safety standards, thereby posing a tangible radiological health risk.

C. Activity concentration index (*I*)

The calculated activity concentration index (*I*) values for the building materials sampled from the Liwale District are detailed in Table 1 (Column 8). The values ranged from 0.1 to 2.9, with an overall average of 0.8. Whilst the average index remains below the internationally recognized safety threshold of $I \leq 1$, suggesting a generally low radiological risk from indoor gamma exposure [23], this aggregate figure requires nuanced interpretation. Notably, Figure 3 illustrates that the average *I* values for sand and gravel are approaching the upper permissible limit.

A granular analysis of the dataset reveals critical exceptions to the average; specifically, 5 out of 25 samples (20%) exceeded the $I \leq 1$ criterion. This subset comprised four sand samples and one gravel sample. Such outliers underscore a significant localized variation that is obscured by the overall average. These elevated values indicate that certain mineral-based materials from the Liwale Districts may lead to indoor external gamma radiation doses exceeding the public limit of 1 mSv y^{-1}. In accordance with IAEA Safety Standard No. SSG-32, building materials with an index exceeding unity ($I > 1$) necessitate rigorous assessment prior to utilization [39]. Consequently, there is a clear imperative for national authorities to establish a formal framework to monitor the radiological suitability of building materials sourced from this region.

D. Annual Effective Dose (E_{ff})

The calculated values of annual effective dose (E_{ff}) across the building materials samples from Liwale District are presented in column 9 of Table 1. The comparative distribution of E_{ff} across the material types is shown in Figure 3, with results ranging from 0.1 to 1.7 mSv y^{-1}, and an overall average of 0.5 mSv y^{-1}. While this average remains below the international recommended public exposure limit of 1 mSv y^{-1}, a sample-specific analysis reveals notable variations.

Specifically, 3 samples comprising 2 sand samples and 1 gravel sample exceeded the 1 mSv y^{-1} safety threshold, representing 12% of the total subset. The occurrence of these elevated values suggests that specific building materials sourced from this region may contribute to an incremental radiological risk for the local population. Consequently, these findings highlight the necessity for targeted regulatory monitoring and the implementation of guidelines to ensure that exposure from natural radioactivity in construction materials is kept as low as reasonably achievable.

4. CONCLUSIONS

This study established that building materials sourced from the Liwale District possess a distinct radiological signature, characterized by elevated levels of ^{226}Ra and ^{232}Th that exceeded global averages, whilst ^{40}K remains within normal limits. The research confirms that these radioactivity levels are primarily lithogenic in origin, directly linked to the region's specific geological composition, predominantly Hypoluvic Arenosols and Luvisols derived from Neogene sandstone deposits.

The assessment of radiological hazard indices indicates that, while the district-wide average poses a low risk to public health, significant sample-specific outliers suggest that certain local materials exceed international safety thresholds. These findings demonstrate that the use of specific lithogenic aggregates in construction could increase indoor gamma radiation exposure. Consequently, this research underscores the importance of implementing systematic radiological screening and quality-control protocols for building-material sources from these geological formations.

Ultimately, this study provides a critical baseline for the radiological mapping of Southern Tanzania. The data serve as a foundation for future investigations into radon exhalation rates and radionuclide transfer into the local food chain, supporting the

development of long-term environmental monitoring and public health protection strategies in the region.

ACKNOWLEDGMENT

We would like to express our sincere gratitude to Prof. Najat Kassim Mohamed for her expert guidance and professional contributions during the proposal development stage of this research.

FUNDING

This research was supported by the Research and Development Section of the Tanzania Atomic Energy Commission (TAEC) under proposal code PR. 084.

CONFLICT OF INTEREST

All authors declare that they have no conflicts of interest.

AUTHOR CONTRIBUTIONS

Mammba, H. P.: Conceptualization, Funding Acquisition, Project Administration, Methodology, Investigation, Formal analysis, Data Curation, Supervision, Writing – original draft. Machibya, M. A.: Validation, Methodology, Software, Investigation, Formal analysis, Visualization, Writing – review & editing.

DATA AVAILABILITY STATEMENT

The authors declare that the data supporting the results of this study are available in the article. Derived data supporting the conclusions of this study are available upon request from the corresponding author.

REFERENCES

[1] KOVLER, K.; TSAPALOV, A.; BOBKIER, R.; WIEGERS, R.; SCHROEYERS, W.; KOVÁCS, T.; TOTH-BODROGI, E.; EL BOUNAGUI, O.; BABCZUK, A. Indoor radon and NORM in building materials: Critical analysis of the current European regulation and road map for the next decade. **J Environ Radioactiv,** Berlin, v. 285, n. 107668, p. 1-8, 2025.

[2] IMANI, M.; ADELIKHAH, M.; SHHROKHI, A.; AZIMPOUR, G.; YADOLLAHI, A.; KOCSIS, E.; TOTH-BODROGI, E.; KOVACS, T. Natural radioactivity and radiological risks of common building materials used in Semnan Province dwellings Iran. **Environ. Sci. Pollut. Res. Int,** Berlin, v. 28, p. 41492-41503, 2021.

[3] ESTOKOVA, A.; SINGOVSZKA, E.; VERTAL, M. Investigation of building materials' radioactivity in a historical building—a case study. **Materials,** Basel, v. 15, n. 19, p. 1-19, 2022.

[4] International Atomic Energy Agency (IAEA). *In*: IAEA. **Regulatory and management approaches for the control of environmental residues containing naturally occurring radioactive material (NORM)**. Vienna, 2006. p. 1-131. ISBN 92-0-113305-7.

[5] MAS, J. L.; RAMIREZ, J. R. C.; BERMUDEZ, S. H.; FERNANDEZ, C. L. Assessment of natural radioactivity levels and radiation exposure in new building materials in Spain. **Radiat Prot Dosimetry,** Oxford, v. 194, n. 2-3, p. 178-185, 2021.

[6] SAMREH, M. M. A.; THABAYNEH, K. H.; KHRAIS, F. W. Measurement of activity concentration levels of radionuclides in soil samples collected from Bethlehem Province, West Bank, Palestine. **Turkish J Eng Env Sci,** Ankara, v. 38, p. 113-125, 2014.

[7] MAMMBA, H.P.; BALOBEGWA, V. A.; MUHULO, A. P.; PANTALEO, P. A.; KAWALA, R. A. Assessment of natural radioactivity and radiation hazards of building

materials in Kinondoni District, Dar es Salaam. **Tanz. J. Sci,** Dar es Salaam, v. 47, n. 2, p. 664-673, 2021.

[8] IDRIS, M. M.; UBAIDULLAH, A.; SULAYMAN, M. B.; ABDULLAHI, B.; SIDI, M. A. Assessment of gamma background exposure levels in some selected residential houses in FCT Abuja, Nigeria. **J. Rad. Nucl. Appl,** Budapest, v. 6, n. 3, p. 245-248, 2021.

[9] WANG, J.; DU, W.; LEI, Y.; CHEN, Y.; WANG, Z.; MAO, K.; TAO, S.; PAN, B. Quantifying the dynamic characteristics of indoor air pollution using real-time sensors: Current status and future implications. **Environment International,** Rio de Janeiro, v. 175, n. 107934, p. 1-12, 2023.

[10] MARTIN, J.G.; KRAAKMAN, N.J.R.; PEREZ, C.; LEBRERO, R.; MUNOZ, R.; A state–of–the-art review on indoor air pollution and strategies for indoor air pollution control. **Chemosphere,** Amsterdam, v. 262, n. 128376, 2021.

[11] FERGUSON, L.; TAILOT, J.; DAVIES, M.; SHRUBSOLE, C.; SYMONDS, P.; DIMITROULOPOULOU, S. Exposure to indoor air pollution across socio-economic groups in high-income countries: A scoping review of the literature and a modelling methodology. **Environment International,** Rio de Janeiro, v. 143, n. 105748, 2020.

[12] United Nations Scientific Committee on the Effects of Atomic Radiation (UNSCEAR), *In*: UNSCEAR, **Sources and effects of ionizing radiation,** Report of the United Nations Scientific Committee on the Effects of Atomic Radiation to the General Assembly, New York: United Nations Publication, 2000. v. 1. ISBN 92-1-142238-8.

[13] International Atomic Energy Commission (IAEA), **Attribution of radiation health effects and inference of radiation risks,** Considerations for Application of the IAEA safety Standards, Safety Report Series No. 122. Vienna: IAEA Publishing Section, 2023.p. 25-39. ISBN 978-92-0-134323-9.

[14] MOHAMMED, K.H.; ZYUGHIR, L.S.; JAAFAR, A.A.; ALMAYAHI, B.A. Biological effect of background radiation and their risk of humans. **Maghreb. J. Pure & Appl. Sci,** Ouja, v. 2, n. 2, p. 71-78, 2016.

[15] RIBEIRO, F.C.A.; LAURIA, D.C.; SILVA, J.I.R.; LIMA, E.S.A.; SABRINHO, N.M.B.A. Baseline and quality reference values for natural radionuclides in soils of Rio de Janeiro State, Brazil. **Rev.Bras.Cienc.Solo,** Viçosa, v. 42, n. e0170146, p. 1-15, 2018.

[16] LEGASU, M. L.; CHAUBEI, A.K. Determination of dose derived from building materials and radiological health related effects from the indoor environment of Dessie city, Wollo, Ethiopia. **Heliyon,** v. 8, n. 3, p. 1-9, 2022.

[17] Directorate-General for Environment (European Commission), **Radiological protection principles concerning the natural radioactivity of building materials**. Radiation Protection 112, EC, STUK Finland, 1999.

[18] International Commission on Radiological Protection (ICRP), SMITH, H. *In*: ICRP, **1990 Recommendations of the international commission on radiological protection**. New York: Pergamon Press, 1991. ISBN 0 08 041144 4.

[19] KASHKINBAYEV, Y.; KAZHIYAKHMETOVA, B.; ALTAEVA, N.; BAKHTIN, M.; TARLYKOV, P.; SAIFULINA, E.; AUMALIKOVA, M.; IBRAYEVA, D.; BOLATOV, A. Radon exposure and cancer risk: Assessing genetic and protein markers in affected populations. **Biology,** Basel, v. 15, n. 506, p. 1-20, 2025.

[20] RESTE, J.; RIMERE, N.; ROMANS, A.; MARTINSONE, Z.; MARTINSONE. I.; VANADZINS, I.; PAVLOVSKA, I. Assessment of indoor radon gas concentration in Latvian households. **Atmosphere,** Basel, v. 15, n. 5, p. 1-12, 2024.

[21] Tanzania Atomic Energy Commission (TAEC). Internal Technical Report: Radiological Survey of Residential Dwellings in Liwale District. Directorate of Radiation Control Unit, Dodoma, Tanzania (Unpublished). 2023.

[22] DONDEYNE, S.; NGATUNGA, E.L.; COOLS, N.; MUGOGO, S.; DECKERS, J. Landscapes and soils of South Eastern Tanzania: their suitability for cashew. Presented at the 19th conference of the Soil Science Society of East Africa, Moshi, 2001.

[23] THE COUNCIL OF THE EUROPEAN UNION (EU). **laying down basic safety standards for protection against the dangers arising from exposure to ionising radiation**, and repealing Directives 89/618/Euratom, 90/641/Euratom, 96/29/Euratom, 97/43/Euratom and 2003/122/Euratom. Official Journal of the European Union, Brussels, 2013.

[24] ILORI, A. O.; CHETTY, N.; ADELEYE, B. Assessment of radiological hazard indices due to natural radionuclides in the soil of Irele Local Government Area, Ondo State, Nigeria. **Environ. Forensics,** London, v. 25, n. 4, p. 173-179, 2023.

[25] LOLILA, F.; MAZUNGA, M. S. Measurements of natural radioactivity and evaluation of radiation hazard indices in soils around the Manyoni uranium deposit in Tanzania. **J. Radiat. Res. Appl. Sci,** Abingdon, v. 16, n. 100524, p. 1-9, 2023.

[26] WANG, Z.; YE, Y. Assessment of Soil radioactivity levels and radiation hazards in Guangyao Village, South China. **J. Radioanal. Nucl,** Bavaria, v. 329, p. 679-693, 2021.

[27] MOSTAFA, A. M. A.; ISSA, S. Natural radioactivity and radiological hazards in some building materials used in new Assiut City, Egypt. **Anglisticum,** Basel, v. 1, n. 1, p. 321-327, 2013.

[28] RANI, A.; SINGH, S. Natural radioactivity in soil samples from some areas of Himachal Pradesh, India using ɤ-ray spectrometry. **Atmos. Environ,** Amsterdam, v. 39, p. 6306-6314, 2005.

[29] HASSAN, N. N.; KHOO, K. S. Measurement of natural radioactivity and assessment of radiation hazard indices in soil samples at Pengerang, Kota Tinggi, Johor. **AIP Publishing,** New York, v. 1584, p. 190-195, 2014.

[30] ISMAIL, A. F.; ABDULLAHI, S.; SAMAT, S.; YASIR, M. S. Radiological dose assessment of natural radioactivity in Malaysian tiles using ResRad-Build computer code. **Saints Malaysiana,** Selangor, v. 47, n. 5, p. 1017-1023, 2018.

[31] BANZI, F. P.; MSAKI, P. K.; MOHAMMED, N. K. Assessment of natural radioactivity in soil and its contributions to population exposure in the vicinity of Mkuju River Uranium Project in Tanzania. **Expert Opin Environ Biol,** London, v. 5, n. 4, p. 1-10, 2017.

[32] Statistician General, National Bureau of Statistics and Office of Chief Government Statistician, Population and Housing Census 2012. **Population distribution by administrative areas,** Dar es Salaam, 2022.

[33] ASADUZZAMAN, K.; MANNAN, F.; KHANDAKER, M. U.; FAROOK, M. S.; ELKEZZA, A.; AMIN, Y. B. M. Assessment of natural radioactivity levels and potential radiological risks of rommon building materials used in Bangladeshi Dwellings. **PLOS ONE,** California, v. 10, p. 1-16, 2015.

[34] JEONG, M.; LEE, K. B.; KIM, K. J.; LEE, M.; HAN, J. Gamma-ray full spectrum analysis for environmental radioactivity by HPGe detector. **J aston Space Sci,** Texas, v. 31, p. 317-323, 2014.

[35] AYENI, D. A.; ADEBIYI, F. M. Evaluation of natural radioactivity and radiation hazards of soils around petroleum products marketing company using gamma ray spectrometry. **Tanz. J. Sci**, Dar es Salaam, v. 48, n. 2, p. 304-312, 2022.

[36] JOEL, E. S.; MAXWELL, O.; ADEWOYIN, O. O.; EHI-EROMOSELE, C. O.; EMBONG, Z.; OYAWOYE, F. Assessment of natural radioactivity in various

commercial tiles used for building purposes in Nigeria. **MethodsX,** Sandtone, v. 5, p. 8-19, 2018.

[37] JEAN-CLAUDE, B.O.; ALFRED, A. D. D.; ALAIN, M. G. Assessment of natural radioactivity in gravel samples collected from Abidjan district in Côte d'Ivoire. **EJAS,** Basel, v. 10, p. 125-134, 2022.

[38] PETOUSSI-HENSS, N.; SATOH, D.; ENDO, A.; ECKERMAN, K. F.; BOLCH, W. E.; HUNT, J.; JANSEN, J. T. M.; KIM, C. H.; LEE, C.; SAITO, K.; SCHLATTL, H.; YEOM, Y. S.; YOO, S. J. International Commission on Radiological Protection (ICRP). *In:* CLEMENT, C. H, FUJITA, H. **Dose Coefficients for external exposure to environmental sources. ICRP Publication 144. Ann. ICRP (49)(2).** Ottawa: SAGE, 2020. p. 29-35. ISBN 9781529741254.

[39] International Atomic Energy Agency (IAEA), *In*: IAEA. **Naturally occurring radioactive materials (NORM VII)**, Vienna, 2015. ISBN 978-92-0-104014-5.

[40] AKRAM, M.; TURKI, I. E. Radiological assessment of hazard index for clay sample in Iraq. **IJONS,** Tamil Nadu, v. 9, p. 16417-16424, 2019.

[41] ZIVUKU, M.; KGABI, N. A.; Tshivhase, V. M. Assessment of radioactivity in particulate matter and soil from selected mining towns of Erongo region, Namibia. **Scientific African,** v. 20, n. e01722, p. 1-10, 2023.

[42] RAVISANKAR, R.; CHANDRAMOHAN, J.; CHANDRASEKARAN, A.; JEBAKUMAR, J. P. P.; VIJAYALAKSHMI, I.; VIJAYAGOPAL, P.; VENKATRAMAN, B. Assessments of radioactivity concentration of natural radionuclides and radiological hazard indices in sediment samples from the East coast of Tamilnadu, India with statistical approach. **Mar. Pollut. Bull,** Qingdao, v. 97, n. 1-2, p. 419-430, 2015.

[43] OSMAN, R.; DAWOOD, Y. H.; MELEGY, A.; EL-BADY, M. S.; SALEH, A.; GAD, A. Distributions and risk assessment of the natural radionuclides in the soil of Shoubra El Kheima, South Nile Delta, Egypt. **MDPI Journal,** Basel, v. 13, n.1, p. 1-16, 2022.

[44] CHEN, T.; ZENG, F.; LIN, C.; YEH, Y.; HUANG, W. Assessment of soil radioactivity associated with risk and correlation with soil properties near Maanshan Nuclear Power Plant, Taiwan. **Applied Sciences,** California, v. 14, n. 20, p. 1-15, 2024.

[45] TURHAN, S. Radiological impacts of the usability of clay and kaolin as raw material in manufacturing of structural building materials in Turkey. **J. Radiol. Prot,** Bristol, v. 29, p. 75-83, 2009.

[46] HARB, S.; EL-KAMEL, A. H.; ZAHRAN, A. M.; ABBADY, A.; AHMED, F. A. Assessment of natural radioactivity in soil and water samples from Aden governorate South of Yemen region. **Int. J. Recent Res. Phys. Chem. Sci,** Lucknow, v. 1, p. 1-7, 2013.

[47] EL-TAHER, A. Assessment of natural radioactivity levels and radiation hazards for building materials used in Qassim area, Saudi Arabia. **Rom. Journ. Phys,** Bucharest, v. 57, n. 3-4, p. 726-735, 2012.

[48] OBORAH, K. A.; HASHIM, N. O.; MIGWI, C. M.; ROTICH, C. Assessment of radioactivity concentration for building materials used in Babadogo Estate, Nairobi City County, Kenya. **Radiat Prot Dosimetry,** Oxford, v. 200, n. 2, p. 201-205, 2023.

[49] KIDANE, Y. B.; DERESSU, T. T.; BELETE, G. D. Evaluation of natural radioactivity level in surface soil from Bambasi district in Benishangul Gumuz region, Ethiopia. **J. Anal. Methods CheM,** New Jersey, v. 2024, p. 1-14, 2024.

LICENSE